Journal of Organometallic Chemistry, 249 (1983) 429–436
Elsevier Sequoia S.A., Lausanne – Printed in The Netherlands

SYNTHESIS OF $[Rh_4(\mu\text{-}PPh_2)_4(\mu\text{-}CO)_2(CO)_4]$ AND CRYSTAL STRUCTURE OF ITS MONOCLINIC FORM

C.P. LAU*,*, C.Y. REN,
Institute of Chemistry, Academia Sinica, Beijing (China)

LANGFORD BOOK and THOMAS C.W. MAK*
Department of Chemistry, The Chinese University of Hong Kong, Shatin, New Territories (Hong Kong)

(Received December 21st, 1982)

Summary

The reaction of $[Rh(CO)_2Cl]_2$ and $LiPPh_2$ in 3:4 molar ratio in tetrahydrofuran afforded the dark brown cluster $[Rh_4(\mu\text{-}PPh_2)_4(\mu\text{-}CO)_2(CO)_4]$, which has been characterized by X-ray analysis. The crystals are monoclinic, space group $P2_1/n$ with $a = 11.985(2)$, $b = 20.577(3)$, $c = 22.345(2)$ Å, $\beta = 96.67(1)°$, $Z = 4$. The structure, refined to $R_F = 0.046$ for 7816 observed Mo-K_α data, is based on a nearly regular tetrahedral Rh_4 skeleton [Rh–Rh bonds vary from 2.758(1) to 2.890(1) Å], four of its six edges being spanned by diphenylphosphide ligands [Rh–P bonds from 2.256(2) to 2.326(2) Å], and the remaining two by doubly-bridging carbonyl groups [Rh–C bonds from 2.001(6) to 2.169(6) Å]. The cluster geometry closely resembles that observed in a recently reported triclinic form of significantly higher density, and differs from it in some Rh–Rh and Rh–P bond distances and the orientations of several peripheral phenyl rings.

Introduction

In the course of a study of the catalytic activities of phosphide-bridged rhodium clusters [1], the synthesis of $[Rh_4(CO)_5(\mu\text{-}PPh_2)_5]^-$ by Meek et al. [2] was duplicated. However, the resulting dark brown solid product exhibited both terminal and bridging CO absorption bands at 2000s, 1972s, 1855ms, and 1802ms cm^{-1}, in disagreement with the all-terminal CO stretching modes (1965, 1950, and 1910 cm^{-1}) for the desired anionic cluster. Repeated trials showed variations in the relative intensities of the observed infrared bands, depending on the rate of mixing

---

* Present address: Department of Applied Science, Hong Kong Polytechnic, Hunghom, Kowloon (Hong Kong).

0022-328X/83/$03.00

of the reactants and the length of the reaction time, thereby suggesting that the product obtained might be a mixture rather than a pure compound.

By altering the $[Rh(CO)_2Cl]_2$ to $LiPPh_2$ molar ratio from 1 : 2 (as specified by Meek et al.) to 3 : 4 and modifying the synthetic procedure, an air-stable dark brown crystalline compound was obtained in good yield. Its infrared spectrum (KBr pellet) indicated the presence of both terminal and bridging carbonyl ligands. Elemental analysis of this compound was consistent with the formulation $[Rh_4(PPh_2)_4(CO)_6]$ (**I**), which we proceeded to characterize by means of X-ray crystallography. While our work was close to completion, we became aware of an alternative synthesis and crystal structure determination of a triclinic form of **I** (henceforth designated as **Ib**) [3]. * In the present paper, we report our analysis of the monoclinic form **Ia**, which has significantly lower density, and compare the molecular structure and packing in the two crystalline modifications.

Experimental

Synthesis

All manipulations were carried out under purified argon in Schlenk reaction vessels. Solvents were dried and degassed before use.

A solution of $LiPPh_2$ [5] (6.86 mmol in 10 ml THF) was slowly dropped into a solution of $[Rh(CO)_2Cl]_2$ (5.15 mmol in 30 ml THF). The solution gradually turned dark reddish brown and was continuously stirred for 30 h. The solvent was then stripped off, and the dark brownish residue loaded into a soxhlet extractor. Hexane was added to the ethereal extract until precipitation just started to appear, and the mixture was allowed to stand at room temperature overnight. The brown powdery precipitate and a small amount of dark brown microcrystals were subsequently filtered off. The mother liquid was allowed to stand at room temperature over a period of several days, during which large dark brown prismatic crystals of **Ia** formed on the wall of the vessel (unoptimized yield: 70%). Infrared spectrum (KBr pellet): 2020ms(sh), 1988s(br), 1861ms, and 1848ms cm^{-1}. Elemental analysis, found: C, 49.02; H, 3.08. $C_{54}H_{40}O_6P_4Rh_4$ calcd.: C, 49.39; H, 3.03%.

X-Ray analysis

A spherically ground crystal of diameter 0.3 mm was mounted on a Nicolet R3m automated four-circle diffractometer. Standard centering and autoindexing procedures indicated a primitive monoclinic lattice, which was subsequently verified by taking axial photographs. The systematic absences, $h0l$ with $(h+l)$ odd and $0k0$ with k odd, established the space group as $P2_1/n$. Accurate unit-cell dimensions were determined from a least-squares fit of 23 reflections ($18° < 2\theta < 26°$). Three standard reflections ($1\ 4\ \bar{2}$, $1\ \bar{4}\ \bar{2}$, and $\bar{1}\ 4\ 2$) monitored every 125 reflections showed only small random fluctuations within $\pm 3\%$, and linear scaling was applied. In addition to Lorentz and polarization factors, absorption correction was applied

(Continued on p. 433)

---

* From decarbonylation and rearrangement of $[Rh_3(\mu\text{-}PPh_2)_3(CO)_5]$ [4] in benzene solution. Space group $P\bar{1}$, $a = 15.855(5)$, $b = 13.861(5)$, $c = 12.747(5)$ Å, $\alpha = 106.79(1)$, $\beta = 99.52(1)$, $\gamma = 99.66(1)°$, $V = 2575.2$ Å^3, $D_c(Z = 2) = 1.70$, $D_m = 1.71$ g cm^{-3}. Blocked-matrix least-squares refinement with the phenyl rings treated as rigid groups and all other atoms varied anisotropically yielded $R_F = 0.067$ and $R_w = 0.080$ for 6978 Mo-$K\bar{\alpha}$ Lp-corrected reflections with $I > \sigma(I)$.

TABLE 1

DATA COLLECTION AND PROCESSING PARAMETERS

Molecular formula	$Rh_4(P(C_6H_5)_2)_4(CO)_6$
Molecular weight	1313.10
Cell constants	$a = 11.985(2)$ Å $b = 20.577(3)$ $c = 22.345(2)$ $\beta = 96.67(1)°$ $V = 5473(1)$ Å $Z = 4$
Density	$D_c = 1.614$, $D_m = 1.63$ g cm^{-3}
Space group	$P2_1/n$
Radiation	graphite-monochromatized Mo-$K\bar{\alpha}$, $\lambda = 0.71069$ Å
Mean μr	0.20
Transmission factors	0.517 to 0.642
Scan type and speed	θ–2θ, 2.55 to 14.65 deg min^{-1}
Scan range	1° below $K_{\alpha 1}$ to 1° above $K_{\alpha 2}$
Background counting	stationary counts for $\frac{1}{2}$ of scan time at each end of scan
Collection range	$h, k, \pm l$; $2\theta_{max} = 50°$
Unique data measured	9384
Observed data with $\lvert F_o\rvert > 2\sigma(\lvert F_o\rvert)$, n	7816
Number of variables, p	277
$R_F = \Sigma\lvert\lvert F_o\rvert - \lvert F_c\rvert\rvert/\Sigma\lvert F_o\rvert$	0.046
Weighting scheme	$w = [\sigma^2(\lvert F\rvert) + 0.0004\lvert F\rvert^2]^{-1}$
$R_w = [\Sigma w(\lvert F_o\rvert - \lvert F_c\rvert)^2/\Sigma w\lvert F_o\rvert^2]^{1/2}$	0.056
Goodness of fit S $= [\Sigma w(\lvert F_o\rvert - \lvert F_c\rvert)^2/(n-p)]^{1/2}$	1.792

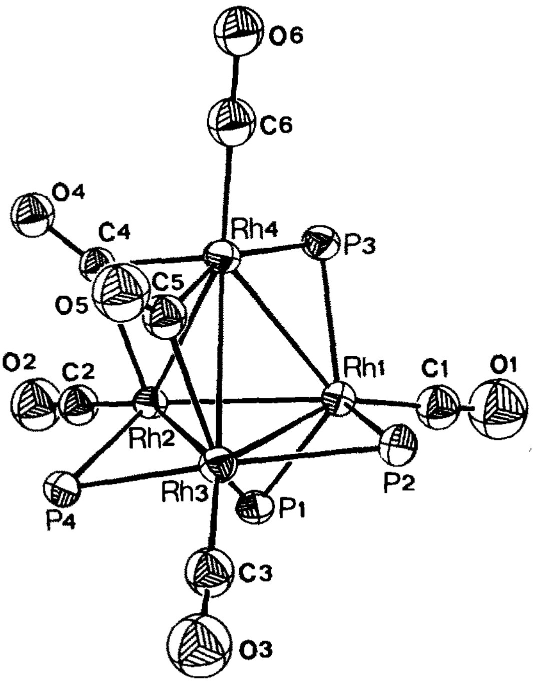

Fig. 1. A perspective view of the stereochemistry of $[Rh_4(\mu\text{-}PPh_2)_4(\mu\text{-}CO)_2(CO)_4]$, **Ia**, showing the atom labelling scheme and thermal ellipsoids at the 30% probability level.

TABLE 2

FRACTIONAL ATOMIC COORDINATES AND ANISOTROPIC THERMAL PARAMETERS ($Å^2 \times 10^3$) FOR Rh, P, AND CARBONYL GROUPS $T = \exp[-2\pi^2\Sigma_i\Sigma_j a_i^\star \cdot a_j^\star h_i h_j U_{ij}]$

Atom	x	y	z	U_{11}	U_{22}	U_{33}	U_{23}	U_{13}	U_{12}
Rh(1)	0.47759(4)	0.15523(2)	0.21822(2)	34.2(3)	33.6(3)	34.0(3)	2.5(2)	5.9(2)	2.1(2)
Rh(2)	0.27952(4)	0.16225(2)	0.26963(2)	29.9(2)	29.0(2)	33.2(2)	2.9(2)	1.5(2)	−1.1(2)
Rh(3)	0.48629(4)	0.18171(2)	0.34570(2)	28.8(2)	31.3(2)	33.6(2)	3.8(2)	2.6(2)	1.1(2)
Rh(4)	0.40084(4)	0.27619(2)	0.25909(2)	32.5(2)	29.4(2)	33.5(2)	4.6(2)	2.5(2)	−0.8(2)
P(1)	0.36804(14)	0.06924(8)	0.24218(7)	42.7(9)	29.0(8)	39.8(9)	0.4(7)	2.8(7)	−0.9(7)
P(2)	0.63211(13)	0.17566(8)	0.28627(7)	30.9(8)	41.4(9)	44.2(9)	3.6(7)	5.8(7)	1.1(7)
P(3)	0.40343(14)	0.24331(8)	0.16169(7)	45.6(9)	39.7(9)	34.9(8)	6.1(7)	5.3(7)	2.2(8)
P(4)	0.30838(13)	0.15916(7)	0.37116(7)	32.1(8)	34.0(8)	34.6(8)	5.4(6)	4.7(6)	1.6(7)
C(1)	0.5388(7)	0.1195(4)	0.1540(3)	77(6)	80(6)	48(5)	−2(4)	15(4)	28(5)
O(1)	0.5761(7)	0.0975(4)	0.1135(3)	148(7)	169(8)	69(4)	−13(5)	46(4)	70(6)
C(2)	0.1297(5)	0.1363(4)	0.2527(3)	32(4)	57(4)	60(5)	2(3)	0(3)	−6(3)
O(2)	0.0397(5)	0.1218(3)	0.2429(3)	45(3)	119(6)	116(5)	2(4)	−8(3)	−19(4)
C(3)	0.5713(5)	0.1666(3)	0.4192(3)	44(4)	36(4)	52(4)	5(3)	2(3)	5(3)
O(3)	0.6227(5)	0.1588(3)	0.4650(2)	73(4)	80(4)	53(3)	14(3)	−19(3)	10(3)
C(4)	0.2384(5)	0.2649(3)	0.2695(3)	31(3)	40(3)	36(3)	2(3)	0(3)	0(3)
O(4)	0.1611(4)	0.2978(2)	0.2726(2)	40(3)	42(3)	73(3)	7(2)	8(2)	7(2)
C(5)	0.4563(5)	0.2818(3)	0.3501(3)	39(4)	39(4)	36(4)	2(3)	1(3)	4(3)
O(5)	0.4749(5)	0.3173(2)	0.3892(2)	88(4)	41(3)	40(3)	−7(2)	−2(2)	6(3)
C(6)	0.4256(5)	0.3652(3)	0.2494(3)	37(3)	43(4)	58(4)	15(3)	3(3)	−5(3)
O(6)	0.4427(5)	0.4186(3)	0.2438(3)	83(4)	38(3)	141(6)	24(3)	14(4)	−14(3)

TABLE 3

BOND LENGTHS [a] (Å) INVOLVING THE Rh AND P ATOMS AND THE CARBONYL GROUPS IN MONOCLINIC $[Rh_4(\mu\text{-}PPh_2)_4(\mu\text{-}CO)_2(CO)_4]$, **Ia**

Rh(1)–Rh(2)	2.758(1) [2.770(1)]	C(1)–O(1)	1.149(11)
Rh(1)–Rh(3)	2.890(1) [2.859(1)]	C(2)–O(2)	1.116(8)
Rh(1)–Rh(4)	2.841(1) [2.872(1)]	C(3)–O(3)	1.143(8)
Rh(2)–Rh(3)	2.866(1) [2.865(1)]	C(4)–O(4)	1.157(7)
Rh(2)–Rh(4)	2.783(1) [2.832(1)]	C(5)–O(5)	1.141(8)
Rh(3)–Rh(4)	2.849(1) [2.824(1)]	C(6)–O(6)	1.128(8)
Rh(1)–P(1)	2.303(2) [2.321(2)]	Rh(1)–C(1)	1.839(8)
Rh(1)–P(2)	2.294(2) [2.283(2)]	Rh(2)–C(2)	1.870(6)
Rh(1)–P(3)	2.326(2) [2.324(3)]	Rh(2)–C(4)	2.169(6)
Rh(2)–P(1)	2.306(2) [2.320(2)]	Rh(3)–C(3)	1.855(6)
Rh(2)–P(4)	2.256(2) [2.261(2)]	Rh(3)–C(5)	2.095(7)
Rh(3)–P(2)	2.318(2) [2.306(2)]	Rh(4)–C(4)	2.001(6)
Rh(3)–P(4)	2.317(2) [2.327(2)]	Rh(4)–C(5)	2.068(6)
Rh(4)–P(3)	2.283(2) [2.264(3)]	Rh(4)–C(6)	1.871(7)

[a] Corresponding bond distances in the triclinic form **Ib** [3] are enclosed in square brackets for comparison.

using an empirical method based on a pseudo-ellipsoidal treatment of reflection intensity measurement at different azimuthal angles. Data collection (at 22°C) and processing parameters are listed in Table 1.

Direct phase determination in space group $P2_1/n$ revealed the positions of the four Rh atoms in the molecule. Other non-hydrogen atoms were found from subsequent difference Fourier maps. The eight phenyl rings were refined as rigid groups (C–C and C–H bonds set to 1.395 and 0.96 Å, respectively), with individual isotropic temperature factors for the carbon atoms and fixed isotropic temperature factors for the hydrogen atoms. All other atoms were varied anisotropically. Blocked-cascade least-squares refinement converged at $R_F = 0.046$ for 7816 observed reflections. The final difference map contained only residues in the neighbourhood of the phenyl rings and showed no diffraction ripples around the Rh and P atoms. Residual maxima and minima in the map fell in the range 1.2 to -0.8 e Å^{-3}.

All computations were performed on a Data General Corporation Nova 3/12 minicomputer with the SHELXTL program package [6,7]. Analytical expressions [8] of neutral atom scattering factors [9] were employed, and anomalous dispersion corrections [10] were incorporated. The final positional and anisotropic thermal parameters for the Rh and P atoms and the carbonyl groups are given in Table 2, in accordance with the atom labelling scheme in Fig. 1. Bond distances involving the Rh and P atoms and the carbonyl groups are given in Table 3. Tables of atomic parameters for the eight phenyl rings *, bond angles *, and structure factors ** are available as supplementary data.

---

* Deposited with Cambridge Crystallographic Data Centre, University Chemical Laboratory, Lensfield Road, Cambridge CB2 IEW, England.

** Obtainable from the authors upon request.

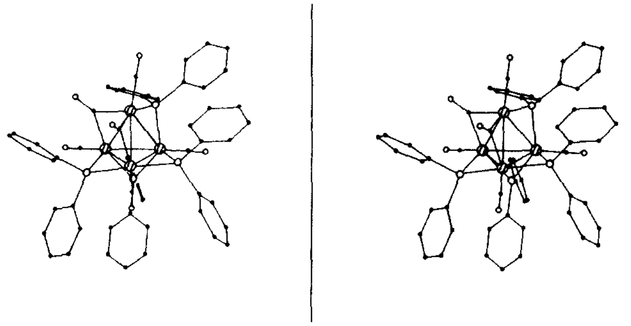

Ia (monoclinic)

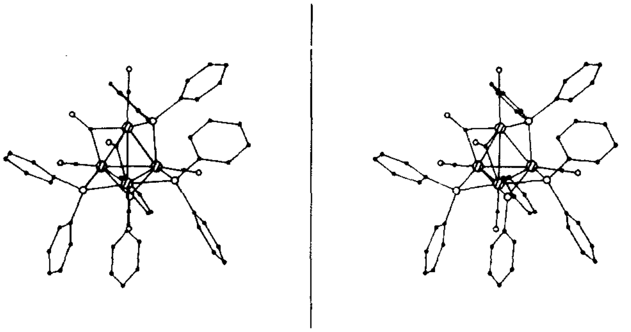

Ib (triclinic)

Fig. 2. Stereoplots of **Ia** and **Ib**, the whole molecule being viewed from exactly the same perspective relative to the Rh_4 unit in each case. Note that the pair of phenyl rings farthest from the observer are approximately parallel in **Ib** but not in **Ia**.

Results and discussion

The present experimental procedure provides a convenient synthesis of the title compound **I** in good yield. An ORTEP plot of the molecule is illustrated in Fig. 1, with all phenyl rings excluded for the sake of clarity. The structure consists of a nearly regular tetrahedral Rh_4 skeleton with four edges bridged by diphenylphosphino ligands and the remaining two by carbonyl groups. Although the central core (comprising the Rh and P atoms and bridging carbonyls) of **I** appears to be invariant in both monoclinic (**Ia**) and triclinic (**Ib**) [3] forms with virtually identical averaged Rh–Rh bond lengths (2.831 and 2.300 Å for **Ia**, and 2.837 and 2.301 Å for **Ib**, respectively), there are significant differences when individual bond distances are compared (Table 3). Furthermore, the orientations of the peripheral phenyl rings are most likely distinguishable, since the density of **Ib** ($D_m = 1.71$ g cm^{-3}) considerably exceeds that of **Ia** ($D_m = 1.63$ g cm^{-3}) as a result of unequal efficiencies in crystal packing. This point has now been verified upon availabity of the atomic coordinates for **Ib** *. The stereoplots in Fig. 2 show that **Ia** and **Ib**, viewed from exactly the same

---

* Courtesy of Dr. R.B. English, personal communication.

TABLE 4

COMPARISON OF BOND DISTANCES (Å) IN THE COMMON Rh_3P_3 UNIT IN SOME TRINUCLEAR AND TETRANUCLEAR CLUSTERS[a]

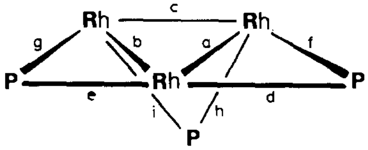

	Ia	Ib	II	III	IV	V
a	2.890(1)	2.859(1)	2.853(2)	2.821(2)	2.806(1)	2.86
b	2.866(1)	2.865(1)	2.815(2)	2.790(2)	2.793(1)	2.78
c	2.758(1)	2.770(1)	2.771(2)	2.744(2)	2.698(1)	2.71
d	2.318(2)	2.306(2)	2.306(5)	2.290(6)	2.263(2)	2.25
e	2.317(2)	2.327(2)	2.320(5)	2.268(6)	2.269(2)	2.27
f	2.294(2)	2.283(2)	2.287(6)	2.323(6)	2.295(2)	2.34
g	2.256(2)	2.261(2)	2.253(5)	2.316(6)	2.288(2)	2.28
h	2.303(2)	2.321(2)	2.315(5)	2.331(5)	2.285(2)	
i	2.306(2)	2.320(2)	2.293(5)	2.332(5)	2.291(2)	

[a] **Ia** = monoclinic form of $[Rh_4(\mu\text{-}PPh_2)_4(\mu\text{-}CO)_2(CO)_4]$, this work,
Ib = triclinic form of $[Rh_4(\mu\text{-}PPh_2)_4(\mu\text{-}CO)_2(CO)_4]$ [3],
II = $[Rh_4(\mu\text{-}PPh_2)_4(\mu\text{-}CO)_2(CO)_3(PPh_3)]$ [11],
III = $[Rh_4(\mu\text{-}PPh_2)_3(CO)_3(PPh_3)_2]$ [12],
IV = $[Rh_3(\mu\text{-}PPh_2)_3(CO)_5]$ [4],
V = $[Rh_3Fe(\mu\text{-}PPh_2)_3(\mu\text{-}CO)_2(CO)_6$ [13], with an approximately planar Rh_3P_2 unit.

perspective, differ mainly in the orientations of the phenyl rings, more noticeably so for the pair farthest from the observer. While **Ib** showed slight statistical disorder of some phosphorus-atom positions, all atoms in **Ia** behave normally in structure refinement and this, coupled with the use of a more extensive dataset ($2\theta_{max} = 50°$) as well as the correction of appreciable absorption effects, accounts for the higher precision achieved in the present analysis.

The tetranuclear rhodium cluster $[Rh_4(\mu\text{-}PPh_2)_4(\mu\text{-}CO)_2(CO)_3(PPh_3)]$, **II** [11], has a structure closely resembling that of **I**, except that the former has a terminal triphenylphosphine ligand attached to the apical Rh(4) atom in place of a carbonyl group in the latter. A survey of the X-ray crystallographic data for several related trinuclear and tetranuclear clusters (Table 4) has revealed a common Rh_3P_3 structural unit comprising a basal Rh_3 triangle with two edges bridged by nearly coplanar phosphorus atoms and the third by a phosphorus atom lying considerably out of this plane. With reference to the atom numbering in Fig. 1, P(2) lies 0.07 Å above the Rh_3 triangle whereas P(4) and P(1) lie below it at 0.50 and 1.80 Å, respectively. The dihedral angles for **Ia** are: Rh(1)Rh(2)-Rh(3)–Rh(1)Rh(3)P(2) = 2.3°, Rh(1)Rh(2)-Rh(3)–Rh(2)Rh(3)P(4) = 16.2° and Rh(1)Rh(2)Rh(3)–Rh(1)Rh(2)P(1) = 103.4°, which closely match the corresponding values of 1.2°, 16.9°, and 103.8° observed for **Ib**. Scrutiny of Table 4 shows that the basic Rh_3P_3 unit deviates markedly from idealized C_s symmetry. The basal Rh_3 triangle is neither regular nor isosceles, and the metal–metal bonds generally follow the order $a > b > c$ except for a reversal a < b in **Ib**. The out-of-plane phosphorus atom is symmetrically bonded to rhodium atoms forming the shortest edge c, whereas the bridging modes involving both in-plane phosphorus atoms are quite asymmetric.

In compound **Ia**, the bridging Rh–C bond lengths vary from 2.001(6) ro 2.169(6) Å and agree well with those in other rhodium clusters [14]. The asymmetry of the bridging is reflected by a difference in the pair of bridging Rh–C bonds up to 0.17 Å. The terminal Rh–C bond lengths vary from 1.839(8) to 1.871(7) Å, which are typical for rhodium-carbonyl clusters [14]. All the C=O bonds, both bridging and terminal, are of similar length [1.116(8) to 1.157(5) Å], and the terminal Rh–C–O groupings are almost linear (bond angles are in the range 178.3–179.2°). All intermolecular contacts correspond to normal Van der Waals interactions.

References

1 C.P. Lau, C.Y. Ren and S.X. Loo, unpublished results.
2 P.E. Kreter, Jr., D.W. Meek and G.G. Christoph, J. Organomet. Chem., 188 (1980) C27.
2 R.B. English, R.J. Haines and N.D.C.T. Steen, S. Afr. J. Chem., 34 (1981) 88.
4 R.J. Haines, N.D.C.T. Steen and R.B. English, J. Organomet. Chem., 209 (1981) C34.
5 A.M. Aguiar, J. Beisler and A. Mills, J. Org. Chem., 27 (1962) 1001.
6 SHELXTL User Manual, Revision 3A, Nicolet XRD Corporation, Fremont, 1982.
7 G.M. Sheldrick in D. Sayre (Ed.), Computational Crystallography, Oxford University Press, New York, 1982, pp. 506–514.
8 D.T. Cromer and J.B. Mann, Acta Crystallogr. A, 24 (1968) 321.
9 International Tables for X-Ray Crystallography, Vol. IV, Kynoch Press, Birmingham, 1973, p. 99.
10 Ref. 9, p. 149.
11 J.D. Jamerson, R.L. Pruett, E. Billig and F.A. Fiato, J. Organomet. Chem., 193 (1980) C43.
12 E. Billig, J.D. Jamerson and R.L. Pruett, J. Organomet. Chem., 192 (1980) C49.
13 R.J. Haines, N.D.C.T. Steen, M. Laing and P. Sommerville, J. Organomet. Chem., 198 (1980) C72.
14 P. Chini, V. Albano and G. Longoni, Advan. Organomet. Chem., 14 (1977) 285.